Int. J. Heat Mass Transfer. Vol. 33, No. 10, pp. 2121–2132, 1990
Printed in Great Britain

0017–9310/90 $3.00 + 0.00

Mixed convection in buoyancy-assisting, vertical backward-facing step flows

J. T. LIN, B. F. ARMALY and T. S. CHEN
Department of Mechanical and Aerospace Engineering, University of Missouri–Rolla, Rolla, MO 65401, U.S.A.

(*Received* 27 *March* 1989 *and in final form* 29 *November* 1989)

Abstract—Mixed convective heat transfer results for laminar, buoyancy-assisting, two-dimensional flow in a vertical duct with a backward-facing step are reported. The present numerical study examines a wide range of inlet flow and wall temperature conditions to cover the domain from pure forced convective flow, where the buoyancy force effects are not present, to the inlet starved convective flow where the buoyancy force effects are significant and where the average inlet velocity is smaller than the corresponding natural convective value. The results compare very favorably with existing, but limited, experimental and numerical data. This study focuses on a backward-facing step geometry with an expansion ratio of 2, but the general observed behaviors are applicable to similar geometries with different expansion ratios. The buoyancy-induced flow decreases the reattachment length and pushes the recirculating region away from the heated wall. Velocity and temperature distributions along with Nusselt numbers and wall friction coefficients are presented for wide ranges of flow and temperature parameters.

INTRODUCTION

IN MANY flows of practical interest the phenomenon of flow separation, due to a sudden expansion in geometry, and the subsequent reattachment, is a common occurrence. The existence of a flow separation and a recirculation region has a significant effect on the performance of heat transfer devices, such as in electronic cooling equipment, cooling passages of turbine blades, combustion chambers, and many other heat exchanger surfaces that appear in engineering designs. Extensive reviews on the fluid flow aspect of separated isothermal flows have been published [1–4]. Reviews dealing with the heat transfer aspects of this flow have been provided by Aung [5, 6], Aung *et al.* [7], Aung and Worku [8], Sparrow *et al.* [9, 10], and Sparrow and Chuck [11]. The published work on this subject did not account, however, for the buoyancy force effects on either the flow or the heat transfer characteristics. These effects become significant in the laminar flow regime where the velocity is relatively low and when the temperature difference is relatively high. This fact has motivated the present study to determine the effects of buoyancy forces on the flow and heat transfer characteristics in separated flows.

Numerical solutions are carried out for laminar mixed convective air flow ($Pr = 0.7$) in a vertical two-dimensional duct with a backward-facing step under buoyancy-assisting flow conditions. Numerical results of interest, such as Nusselt numbers, velocity and temperature distributions, reattachment lengths, and friction coefficients are presented for the purpose of illustrating the effects of the buoyancy force on these parameters.

ANALYSIS

Consider a two-dimensional, laminar convective flow in a vertical duct with a sudden expansion behind a backward-facing step of height s as shown in Fig. 1. The straight wall of the duct is maintained at a uniform temperature that is equal to the inlet air temperature T_o. The stepped wall downstream of the step is heated to a uniform temperature that can be adjusted to any desired value T_w. The upstream portion of the stepped wall and the backward-facing step are treated in this study as adiabatic surfaces. The inlet upstream length of the duct is x_i and the exit downstream length of the duct is x_e. These lengths are considered infinite but the calculation domain is limited to a length of $L_e = x_e + x_i$. The smaller section of the duct upstream of the step has a height h and the larger section downstream of the step has a height $H = h + s$. Air flows upward into the duct at an average inlet velocity of u_o and a uniform temperature of T_o. The gravitational acceleration g is acting vertically downward.

By employing the constant property assumption and the Boussinesq approximation, the non-dimensional form of the governing conservation equations for the physical problem described can be written as

$$\frac{\partial U}{\partial X} + \frac{\partial V}{\partial Y} = 0 \tag{1}$$

$$U\frac{\partial U}{\partial X} + V\frac{\partial U}{\partial Y} = -\frac{\partial P}{\partial X} + \frac{1}{Re_s}\left(\frac{\partial^2 U}{\partial X^2} + \frac{\partial^2 U}{\partial Y^2}\right) + \frac{Gr_s}{Re_s^2}\theta \tag{2}$$

NOMENCLATURE

A	cross-sectional area
C_f	friction coefficient, $\tau_w/(\rho u_o^2/2)$
F_k	net force due to differences in kinetic energy, $\int_A [(\rho u^2)_e - (\rho u^2)_o]\, dA/2$
F_p	net force due to differences in pressure, $\int_A (p_o - p_e)\, dA$
g	gravitational acceleration
Gr_s	Grashof number based on the step height, $g\beta(T_w - T_o)s^3/\nu^2$
h	channel height at inlet
H	channel height at exit
Nu_s	local Nusselt number, as defined by equation (7) or equation (8)
p	pressure
P	dimensionless pressure, $(p+\rho g x)/(\rho_o u_o^2)$
Pr	Prandtl number
Re_s	Reynolds number based on the step height, $u_o s/\nu$
s	step height
T	temperature
T_b	bulk temperature
T_o	inlet temperature
T_w	temperature of heated wall
u	streamwise velocity component
u_i	local inlet velocity
u_o	average inlet velocity
U	dimensionless streamwise velocity component, u/u_o
v	transverse velocity component
V	dimensionless transverse velocity component, v/u_o
x	streamwise coordinate as measured from the step
x_e	calculation domain downstream of step
x_f	reattachment length of forced convective flow
x_i	inlet length upstream of step
x_n	location of peak Nusselt number
x_o	secondary recirculation length
x_r	reattachment length
X	dimensionless streamwise coordinate, x/s
X_e, X_i, X_n, X_o, X_r	$x_e/s, x_i/s, x_n/s, x_n/s, x_o/s, x_r/s$
y	transverse coordinate
Y	dimensionless transverse coordinate, y/s.

Greek symbols

β	volumetric expansion coefficient
θ	dimensionless temperature, $(T-T_o)/(T_w-T_o)$
ν	kinematic viscosity
ξ	buoyancy force parameter, $Gr_s/Re_s^2 = g\beta(T_w-T_o)s/u_o^2$
ρ_o	density at inlet
τ_w	local wall shear stress, $\mu(\partial u/\partial y)_w$.

Subscripts

e	exit conditions
o	inlet conditions
w	wall conditions.

$$U\frac{\partial V}{\partial X} + V\frac{\partial V}{\partial Y} = -\frac{\partial P}{\partial Y} + \frac{1}{Re_s}\left(\frac{\partial^2 V}{\partial X^2} + \frac{\partial^2 V}{\partial Y^2}\right) \quad (3)$$

$$U\frac{\partial \theta}{\partial X} + V\frac{\partial \theta}{\partial Y} = \frac{1}{Pr\, Re_s}\left(\frac{\partial^2 \theta}{\partial X^2} + \frac{\partial^2 \theta}{\partial Y^2}\right). \quad (4)$$

The dimensionless parameters in the above equations are defined by

$$U = u/u_o, \quad V = v/u_o, \quad X = x/s, \quad Y = y/s$$
$$\theta = (T-T_o)/(T_w-T_o), \quad P = (p+\rho g x)/\rho_o u_o^2$$
$$Pr = \nu/\alpha, \quad Re_s = u_o s/\nu, \quad Gr_s = g\beta(T_w-T_o)s^3/\nu^2. \quad (5)$$

The thermal diffusivity α, kinematic viscosity ν, and thermal expansion coefficient β are evaluated at the film temperature $T_f = (T_o+T_w)/2$.

The boundary conditions for the above set of equations are given below.

(a) Upstream inlet conditions

at $X = -X_i$ and $1 \leqslant Y \leqslant H/s$:

$$U = u_i/u_o, \quad V = 0, \quad \theta = 0 \quad (6a)$$

where u_i is the local inlet velocity distribution which is taken as having a parabolic profile and u_o the average inlet velocity; that is, u_i/u_o is given by

$$u_i/u_o = 6[-y^2 + (H+s)y - Hs]/(H-s)^2. \quad (6b)$$

(b) Downstream exit conditions

at $X = X_e$ and $0 \leqslant Y \leqslant H/s$:

$$\partial U/\partial X = 0, \quad \partial^2\theta/\partial X^2 = 0$$
$$\partial V/\partial X = 0 \quad (6c)$$

along with an overall mass conservation check at the exit.

(c) Straight wall

at $Y = H/s$ and $-X_i \leqslant X \leqslant X_e$:

$$U = 0, \quad V = 0, \quad \theta = 0. \quad (6d)$$

(d) Stepped wall

Upstream of the step

at $Y = 1$ and $-X_i \leqslant X < 0$:

$$U = 0, \quad V = 0, \quad \partial\theta/\partial Y = 0. \quad (6e)$$

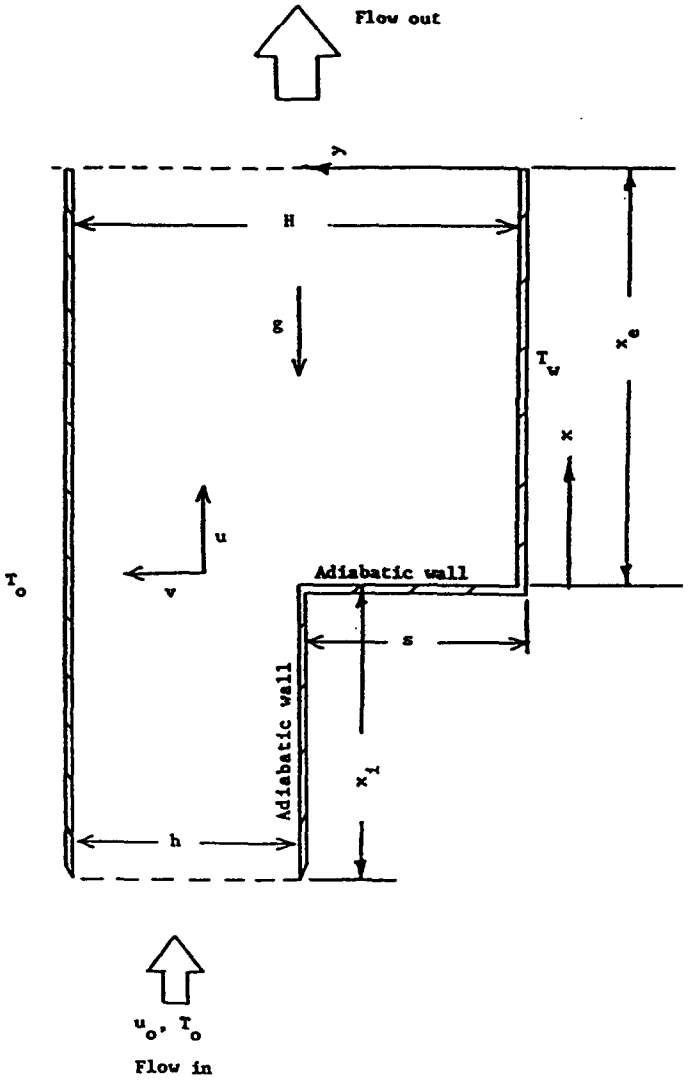

FIG. 1. Schematic diagram.

At the step

$$\text{at } X = 0 \text{ and } 0 \leqslant Y \leqslant 1:$$

$$U = 0, \quad V = 0, \quad \partial\theta/\partial X = 0. \tag{6f}$$

Downstream of the step

$$\text{at } Y = 0 \text{ and } 0 < X \leqslant X_e:$$

$$U = 0, \quad V = 0, \quad \theta = 1. \tag{6g}$$

The last term on the right-hand side of equation (2) represents the buoyancy force contribution which has not been examined previously in the open literature. The downstream length, x_e, of the calculation domain was chosen to be 70 steps (i.e. $X_e = 70$). Calculations have verified that the flow becomes fully developed before the end of this section. The upstream length of the calculation domain, x_i, was chosen to be 5 steps (i.e. $X_i = 5$) and the velocity profile at the inlet section was specified as parabolic, equation (6b), and its temperature was chosen as uniform at T_o.

The solution of the governing set of coupled partial differential equations was obtained by using a finite difference scheme, embodied in the computer code TEACH using the SIMPLE algorithm. The solution procedure started by supplying initial estimates for the velocity, temperature, and pressure fields and a converged solution was obtained by iteration. The momentum equations were used first in the iteration process, using the estimated temperature for the buoyancy force calculations, and then the energy equation was used to upgrade the temperature, and this process was repeated for each iteration step until a converged solution was reached.

The grid distribution in the calculation domain was nonuniform in both the longitudinal and the crossflow coordinate directions. A large number of grid points were placed in the areas where steep variations of velocities were expected, i.e. near the step and near the reattachment length in the x coordinate direction, and near the walls of the duct in the y coordinate

direction. Some of this information was deduced from preliminary calculations using equally spaced grids. Solutions were performed with different grid densities and the required grid number for ensuring grid-independent solutions was determined for different Reynolds numbers. It was found that for the range of parameters examined in this study, $Re_s < 200$, a grid density of $Nx \times Ny = 120 \times 50$ is sufficient for providing a grid-independent solution. A smaller grid and a higher grid density of 250×70 was used to assure a grid-independent solution. The computer program was run on a CRAY X/MP supercomputer, and the solution converged in less than 1000 iterations while utilizing approximately 1–3 min of CPU.

RESULTS AND DISCUSSION

The computer code and the numerical scheme were used to check the fluid flow measurements of Armaly *et al.* [4], the predicted Nusselt numbers of Sparrow and Chuck [11], and the analytically predicted velocity and temperature distributions of Aung and Worku [8]. This step was used to validate the numerical scheme and the convergence criterion that were used in this study. Figures 2(a) and (b) provide a comparison between the present predicted results without the buoyancy force effect and the measurements of ref. [4] for two Reynolds numbers $Re_s = 195$ and 50 at various downstream locations from the backward-facing step. This backward-facing step geometry has an expansion ratio of 1.94 and a step height of 0.49 cm. As can be seen from the figures, the agreement between the predicted and measured results is excellent with the exception at the location $X = 2.55$ for both Reynolds numbers. This downstream location is in the recirculating region of the flow and, as stated in ref. [4], the flow starts to develop a three-dimensional behavior in the neighborhood of the reattachment region in the experimental geometry for $Re_s > 200$. The predicted and the measured reattachment lengths of ref. [4] start to deviate from each other at Reynolds numbers higher than 200 ($Re_s \geq 200$), thus placing an upper limit on the good agreement between the predicted and measured results from that study. The measured results for $Re_s = 50$ at $X = 2.25$ appear not to satisfy the conservation of mass and thus could potentially be reflecting some experimental errors inside the recirculation region where the velocity is negative and its magnitude is very small.

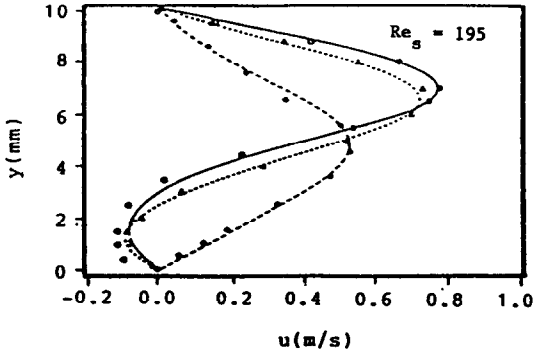

FIG. 2(a). Comparison of predicted velocity profiles with measurements (Armaly *et al.* [4]: ○○○, $X = 2.55$; △△△, $X = 4.18$; ◇◇◇, $X = 11.07$).

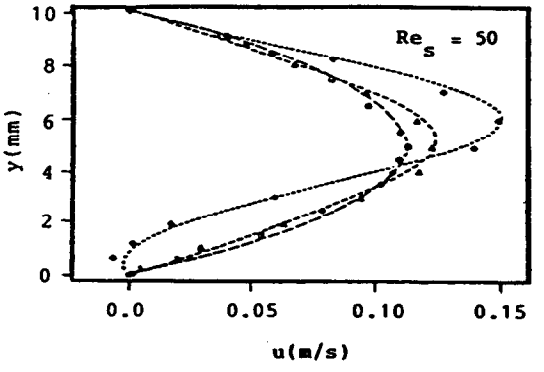

FIG. 2(b). Comparison of predicted velocity profiles with measurements (Armaly *et al.* [4]: ◇◇◇, $X = 2.55$; △△△, $X = 4.18$; ○○○, $X = 12.04$).

The computer code was also utilized to predict the pure forced convection Nusselt numbers for the conditions that were studied by Sparrow and Chuck [11]. A comparison between the two results is shown in Fig. 3 for three different expansion ratios (with the step height remaining constant at 0.48 cm). The agreement between the two studies appears to be very good for the smaller H/s ratios, but deteriorates slightly for the large H/s case. This deterioration could be due to the need for using a larger number of mesh points in the calculation domain in the earlier study for ducts with a larger expansion ratio.

Additionally, the analytical results of Aung and Worku [8] for the fully developed laminar mixed convection flow in a two-dimensional, asymmetrically heated vertical duct were utilized for comparison with the present numerically predicted values. The fully developed mixed convection duct flow behavior is expected to appear in this backward-facing step geometry at a downstream location that is far away from the step. Numerically predicted velocity and temperature distributions at these downstream locations provided excellent agreement with the analytical results of Aung and Worku [8] for fully developed mixed convection duct flow.

The good agreements with existing results for various flow geometries and temperature conditions demonstrated above provided the authors with a measure of confidence for using the numerical scheme to examine the influence of buoyancy force on the flow and the heat transfer characteristics of separated flows, a problem for which measurements or predictions are not available in the literature.

In this study attention is focused on a specific backward-facing step geometry, with an expansion ratio of two ($H/h = 2.0$) and a step height of 0.48 cm, in

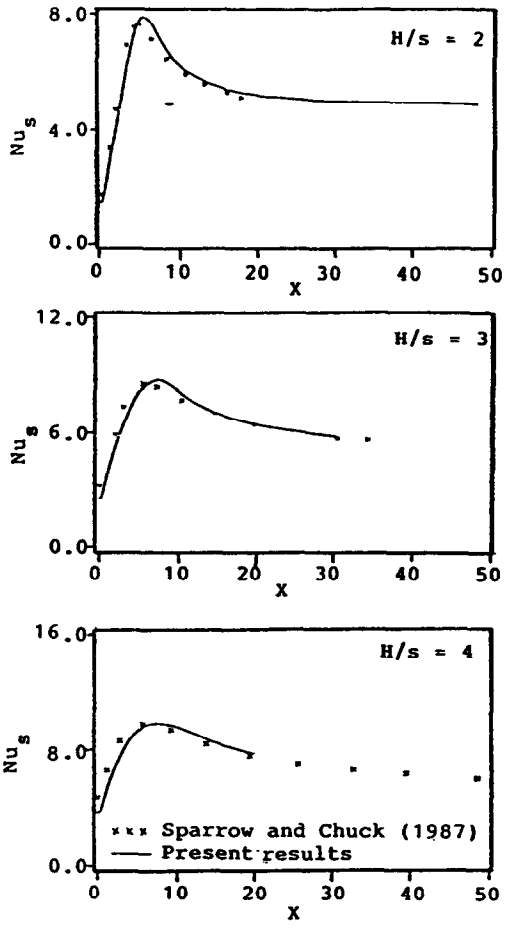

FIG. 3. Comparison of predicted Nusselt numbers with those predicted by Sparrow and Chuck [11] for $Re_s = 100$ and $s = 0.48$ cm.

a buoyancy-assisting, two-dimensional vertical duct flow. This geometry is identical to the one used in ref. [4]. The straight wall of the duct is maintained at the inlet air temperature of 20°C, while the stepped wall of the duct is maintained adiabatic for the upstream section of the step and for the step itself. The downstream section behind the step is maintained at a higher, but uniform, temperature.

The general flow characteristics as affected by increasing the wall temperature (increasing the buoyancy force) is clearly shown in Fig. 4 for a Reynolds number Re_s of 50 with $(T_w - T_o)$ of 1–75°C. These figures capture only a small region of the calculation domain to highlight the influence of buoyancy forces on the recirculation region. They illustrate the stream function behavior for a fixed inlet Reynolds number of $Re_s = 50$, for six levels of wall temperature difference $(T_w - T_o) = 1$, 12.5, 37.5, 43.75, 50, and 75°C. The flow separates behind the backward-facing step and reattaches to the heated wall, thus forming a recirculation region between the step and the heated wall. As the wall temperature increases, the reattachment length decreases and the size of the secondary, inner recirculation region that develops at the corner between the heated wall and the step, increases. This trend continues until the secondary recirculation region is sufficiently strong to lift the main recirculation region away from the heated wall, and thus venting itself to the main flow. At that point the main recirculation region is detached from the heated wall and attaches itself to the step. An increase in the Reynolds number for a fixed wall temperature will decrease the buoyancy parameter, Gr_s/Re_s^2, and will delay the above observed flow behavior to a higher wall temperature.

The behaviors of the reattachment length and the friction coefficient are shown in Figs. 5 and 6, respectively, to illustrate how they are affected by the buoyancy force. The buoyancy induced flow in the streamwise direction and adjacent to the heated wall decreases the reattachment length x_r with increasing $(T_w - T_o)$ or decreasing Re_s, as shown in Fig. 5. Figure 6 illustrates that for $Re_s = 50$ and $(T_w - T_o) > 50$°C the reattachment of the flow to the heated wall no longer exists, and the friction coefficient, C_f, remains positive for all downstream locations after the step.

As the wall temperature difference $(T_w - T_o)$ increases for a fixed Reynolds number the flow characteristics change from forced convective flow to an inlet starved convective flow. Starved flow is designated as one with average inlet velocity that is smaller than what could be achieved if the duct was operated in the natural convective flow mode, i.e. unrestricted inlet flow rate. Under these starved flow conditions, a reversed flow could develop from the downstream section of the duct along the cooler wall as described by Aung and Worku [8]. An approximate criterion for the occurrence of the starved flow condition can be found by comparing the net force resulting from the pressure difference across the calculation domain, F_p, to the net force resulting from the changes of the kinetic energy across the calculation domain, F_k. If the force resulting from the pressure drop is larger than the force resulting from changes in the kinetic energy then the flow is forced, and if it is smaller then the flow is starved. Natural convective flow corresponds approximately to the case when the two forces are equal to each other. This criterion is illustrated in Fig. 7 for Reynolds numbers of 50 and 100. The results in Figs. 7 and 4 show that the disappearance of the reattachment from the heated wall will occur only in the starved flow regime. Figure 7 illustrates that for the geometry considered in this study, starved flow conditions will occur for $Re_s = 50$ when $(T_w - T_o) \geqslant 17$°C, and for $Re_s = 100$ when $(T_w - T_o) \geqslant 37.5$°C. These conditions correspond to $Gr_s/Re_s^2 \geqslant 0.095$ and 0.048, respectively. The results in Fig. 7 for the two Reynolds numbers collapse into one line if they are plotted against Gr_s/Re_s. From that plot one can deduce that the starved flow conditions occur when $Gr_s/Re_s > 5$ for this geometry.

The effects of buoyancy forces on the velocity and temperature distributions are presented in Figs. 8 and 9, respectively, for $Re_s = 50$, at three different cross

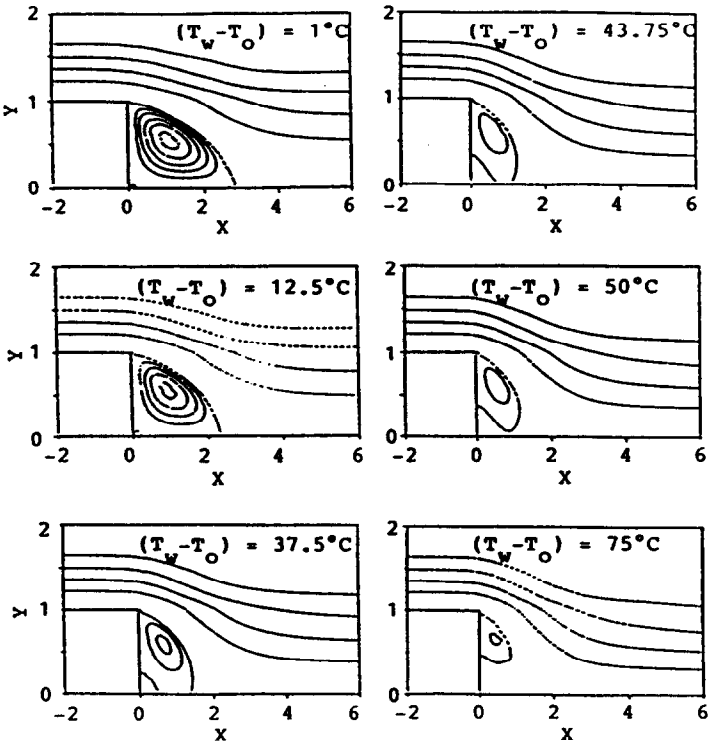

FIG. 4. Effects of buoyancy force on stream lines, $Re_s = 50$ ($s = 0.48$ cm, $H/h = 2.0$).

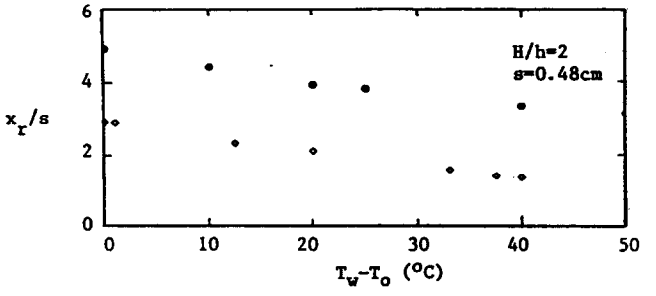

FIG. 5. Effects of buoyancy parameter on reattachment length (◇◇, $Re_s = 50$; ⊙⊙, $Re_s = 100$).

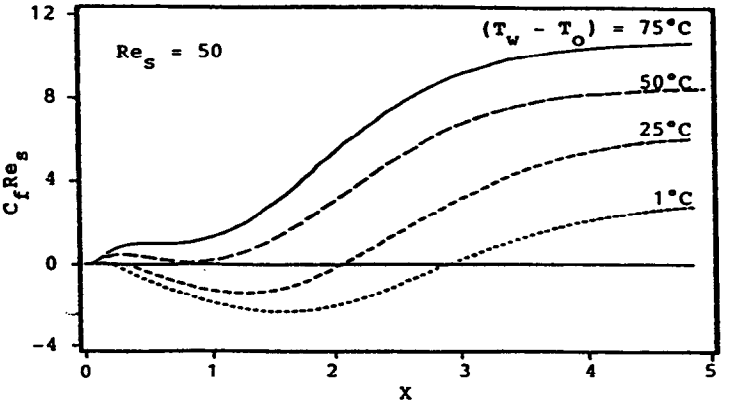

FIG. 6. Buoyancy effects on friction coefficient ($s = 0.48$ cm, $H/h = 2.0$).

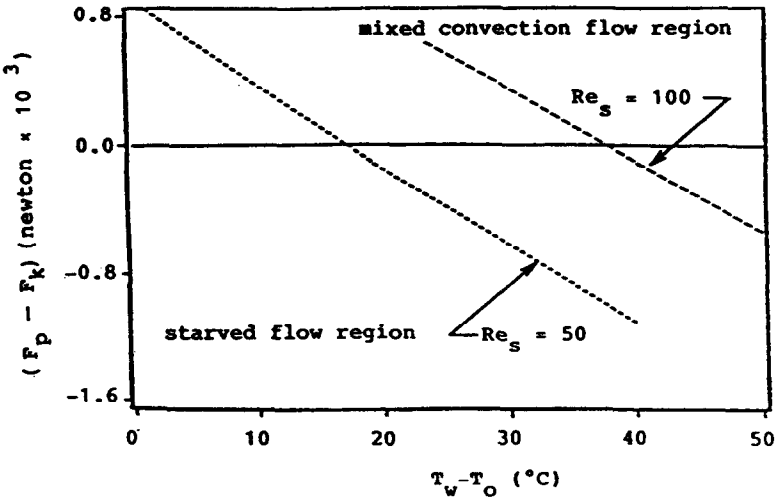

FIG. 7. Criteria for starved flow ($s = 0.48$ cm, $H/h = 2.0$).

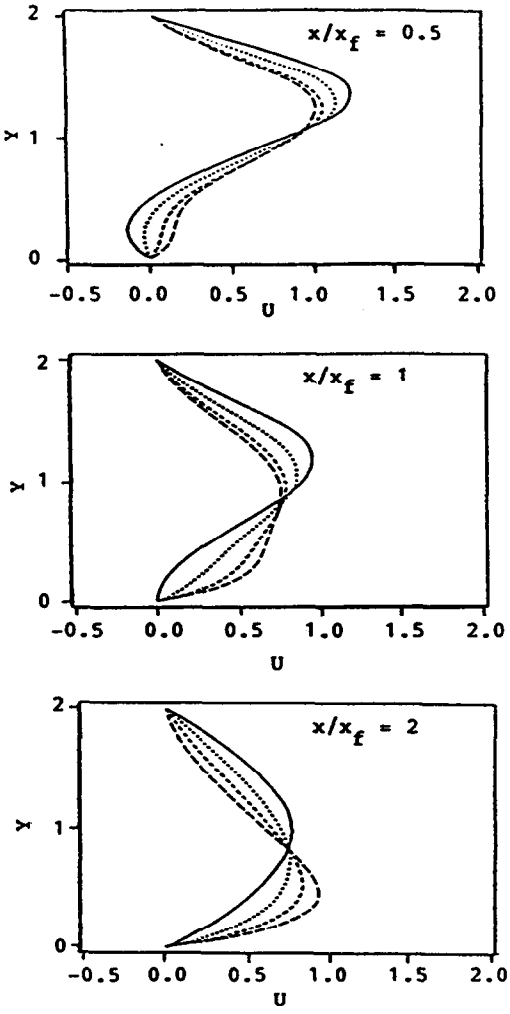

FIG. 8. Buoyancy effects on velocity distribution for $Re_s = 50$: ——, $\Delta T = 1$°C; ·····, $\Delta T = 25$°C; ----, $\Delta T = 50$°C; – – –, $\Delta T = 75$°C and $X_f = 2.91$ ($s = 0.48$ cm, $H/h = 2.0$).

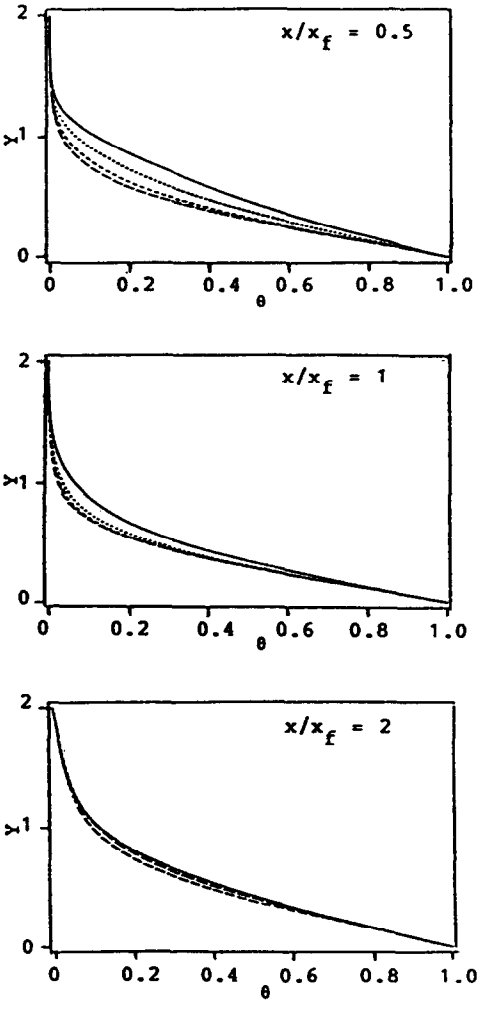

FIG. 9. Buoyancy effects on temperature distribution for $Re_s = 50$: ——, $\Delta T = 1$°C; ·····, $\Delta T = 25$°C; ----, $\Delta T = 50$°C; – – –, $\Delta T = 75$°C and $X_f = 2.91$ ($s = 0.48$ cm, $H/h = 2.0$).

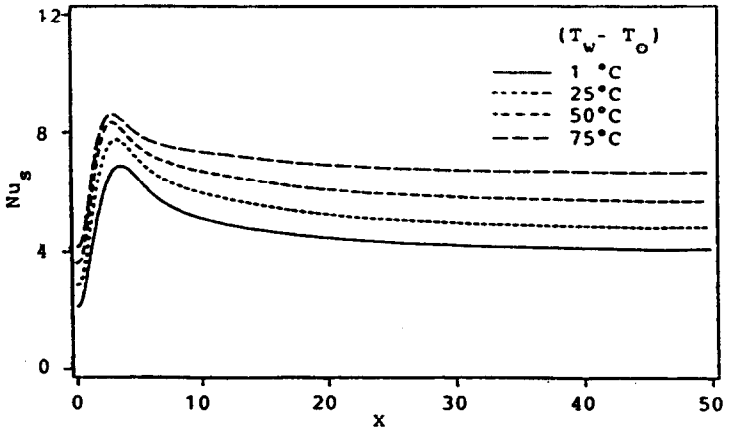

FIG. 10. Buoyancy effects on Nusselt number for $Re_s = 50$ ($s = 0.48$ cm, $H/h = 2.0$).

sections $x/x_f = 0.5$, 1, and 2, where x_f is the reattachment length for isothermal flow and is calculated to be $X_f = 2.91$. It is clear from Fig. 8 that the effect of the buoyancy force on the velocity distribution is significant. The accelerated flow near the heated wall pulls the velocity profile toward that wall, and that trend increases as the wall temperature increases. Increased wall temperature will also decrease the reattachment length, reduce the size of the main recirculation region, and increase the temperature gradient (heat transfer) at the heated wall, particularly in the recirculation region (see Fig. 9). These effects are less pronounced outside the recirculation region, where the temperature distribution develops slowly as the distance from the step increases until it reaches its fully developed linear distribution form.

The effect of buoyancy forces on the Nusselt number is illustrated in Fig. 10 for a Reynolds number, Re_s, of 50. The Nusselt number is defined in terms of the average bulk temperature and the step height as follows:

heated wall

$$Nu_s = [(-k\,\hat{c}T/\hat{c}y)_{y=0}]s/[k(T_w - T_b)] = [(T_w - T_o)/(T_w - T_b)](-\hat{c}\theta/\hat{c}Y)_{Y=0}; \quad (7)$$

cool wall

$$Nu_s = [(-k\,\hat{c}T/\hat{c}y)_{y=H}]s/[k(T_b - T_o)] = [(T_w - T_o)/(T_b - T_o)](-\hat{c}\theta/\hat{c}Y)_{Y=H/s}. \quad (8)$$

The Nusselt number is seen to increase as the wall temperature increases and, although not shown for the case of $Re_o = 100$ to conserve space, the influence of wall temperature on the Nusselt number decreases as the Reynolds number increases. The Nusselt number curves have the normal peaks that are associated with separated flow and the peak point occurs downstream of the reattachment point. In addition, the Nusselt number curves for the boundary conditions considered in this study, have a minimum at the corner of the step as predicted by Sparrow and Chuck [11].

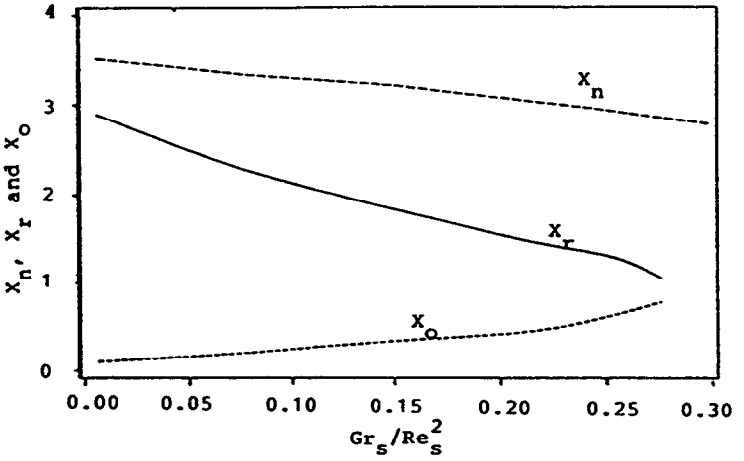

FIG. 11. Effects of buoyancy parameter on reattachment length X_r, secondary circulation length X_o and location of maximum heat transfer X_n, $Re_s = 50$ ($s = 0.48$ cm, $H/h = 2.0$).

It should be noted that the peak in the Nusselt number distribution continues to occur even after the disappearance of the reattachment point from the heated wall (see Fig. 4 for $Re_s = 50$ and $(T_w - T_0) > 50°C$). The Nusselt number increases from its minimum value at the corner of the step to its peak value in the neighborhood of the reattachment point, then decreases slowly to its fully developed value as the distance from the step increases. The Nusselt number increases almost linearly from its minimum to its maximum values and at approximately the same rate as the temperature difference $(T_w - T_0)$ or the buoyancy parameter Gr_s/Re_s^2 increases. The neglect of the buoyancy force effect in predicting the peak Nusselt number could lead to an error of underestimation by over 30%. The increase in the Nusselt number with increasing wall temperature is attributed in part to the increase in the bulk fluid temperature, equation (7), which increases rapidly near the step and levels slowly to its fully developed value downstream. The magnitude of the bulk temperature increases as the wall temperature increases.

Figure 11 displays the behavior of three different length parameters as measured from the step for $Re_s = 50$. The first is the reattachment length, $X_r = x_r/s$, of the main recirculation region, the second is the length, $X_o = x_o/s$, of the secondary recirculation region that develops at the corner, and the third length, $X_n = x_n/s$, identifies the location of the peak Nusselt number. Both the peak Nusselt number length, X_n, and the reattachment length of the main recirculation region, X_r, decrease, while the length of the secondary recirculation region, X_o, increases as the value of the buoyancy parameter increases. The peak Nusselt number occurs downstream of the reattachment point (i.e. $X_n > X_r$) and the spacing

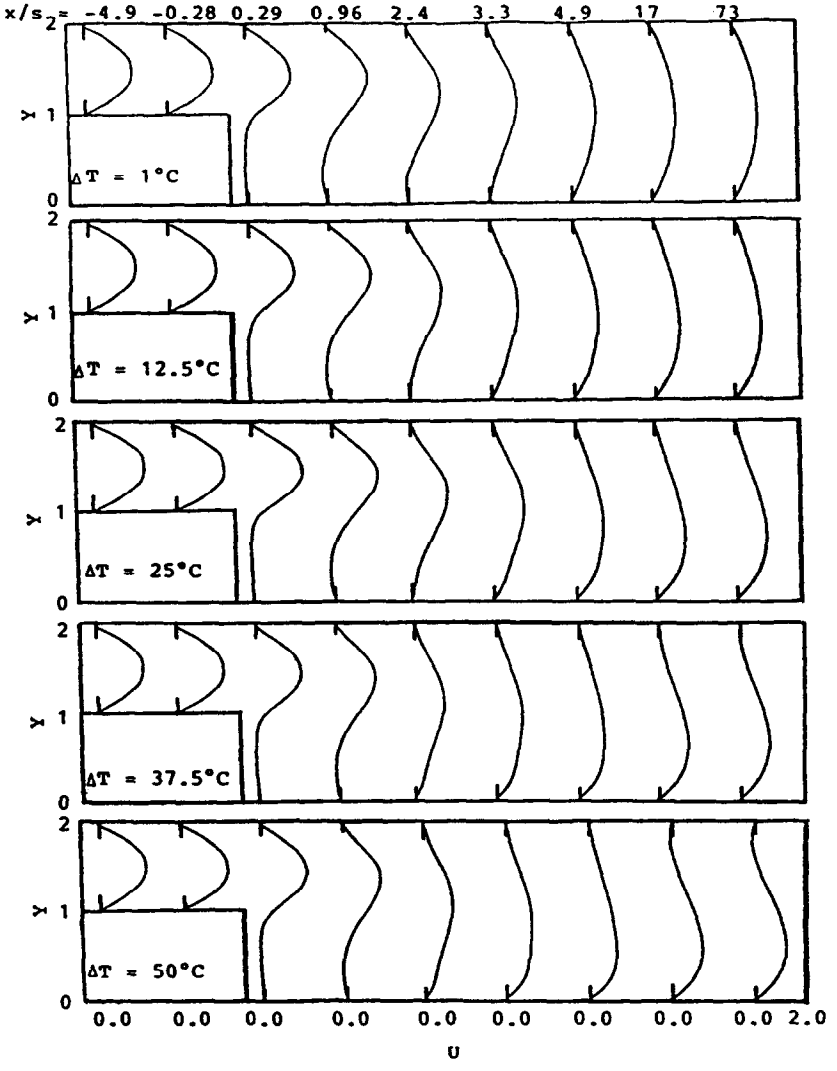

FIG. 12. Dimensionless velocity profiles along the streamwise direction for $Re_s = 50$, and for different wall temperatures ($s = 0.48$ cm, $H/h = 2.0$).

$(X_n - X_r)$ increases as the buoyancy parameter increases.

The developments of the velocity and the temperature profiles throughout the calculation domain are shown, respectively, in Figs. 12 and 13. These two figures display the general behavior of the velocity and the temperature profiles at several downstream locations for several wall temperature differences (i.e. buoyancy force intensities) for a Reynolds number of 50. The velocity profile develops from its inlet parabolic distribution to its fully developed distribution far downstream from the step (Fig. 12). The fully developed velocity distribution, however, is different for different values of the buoyancy parameter, and could include regions of reversed flow as discussed by Aung and Worku [8] and as can be seen for $Re_s = 50$ and $(T_w - T_0) > 37.5°C$. Similarly, the temperature profile develops through the separation region from its inlet uniform distribution to its fully developed linear distribution far downstream from the step (Fig. 13).

For a starved flow condition, a reversed flow develops from the downstream section of the duct and penetrates along the cool wall to feed the flow and to balance the induced buoyancy force. The penetration depth of the reversed flow increases as the buoyancy force increases. In the limit when the inlet flow is reduced to zero, the geometry becomes equivalent to an open cavity where recirculating flow drives the convection inside the cavity. The authors believe that in actual starved flow conditions in this geometry, the flow will start to exhibit a three-dimensional behavior and possible transition to turbulent flow may follow. This will make the laminar two-dimensional solution

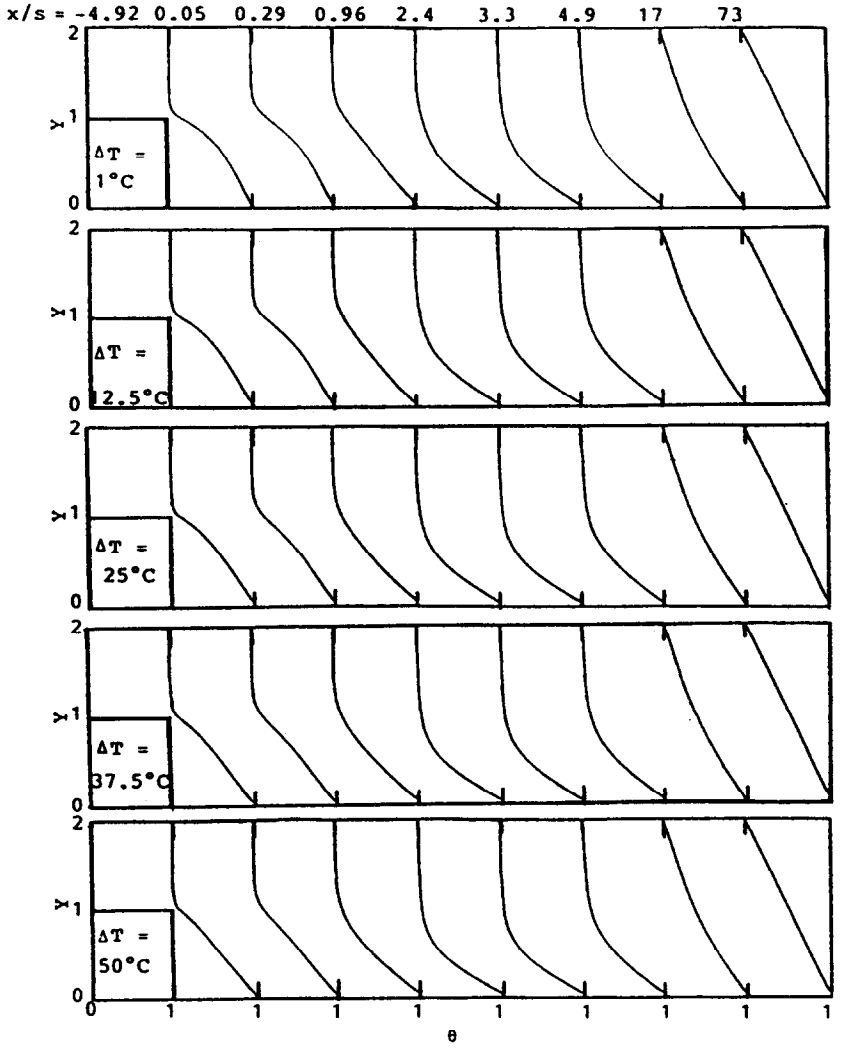

FIG. 13. Dimensionless temperature profiles along the streamwise direction for $Re_s = 50$, and for different wall temperatures ($s = 0.48$ cm, $H/h = 2.0$).

not useful for that range of conditions. Experimental observations, which will be pursued by the authors, are needed to determine when that transition will occur.

CONCLUSIONS

The significant effects that the buoyancy force has on the heat transfer in laminar flow inside a vertical duct with a backward-facing step were demonstrated and quantified in this numerical study. The full range of mixed convective flow, from the pure forced convective flow to the inlet starved convective flow, was examined. As expected, the influence of the buoyancy force on the velocity distribution is more pronounced than its influence on the temperature distribution. The buoyancy force changes significantly the shape of the main recirculation region behind the step and causes the reattachment length to decrease as its magnitude increases. A secondary recirculation region develops at the corner of the step and grows as the buoyancy force increases until it vents itself to the main flow by pushing the main recirculation region away, thus leaving the heated wall without any reattached flow region. This behavior appears to occur only for the inlet starved flow condition under which transition to three-dimensional or turbulent flow behavior could occur, thus invalidating the present two-dimensional laminar flow results for that regime. The Nusselt number, defined in terms of the bulk-wall temperature difference, exhibits the normal peak value that occurs downstream of the reattachment point and a minimum value that occurs at the corner of the step. Both the peak value and the minimum value of the Nusselt number increase as the value of the buoyancy parameter increases. The present numerical study assumes that laminar flow exists for the entire range of parameters that were examined, and experimental verification of this assumption is needed, which will be undertaken in a future study by the authors.

Acknowledgement—The authors wish to acknowledge the support of the National Center for Computing Applications at the University of Illinois for providing access to the GRAY X-MP Computer under grant number CAT880010N.

REFERENCES

1. B. F. Armaly and F. Durst, Reattachment length and recirculation regions downstream of two dimensional single backward facing step. In *Momentum and Heat Transfer Process in Recirculating Flows*, ASME HTD-Vol. 13, pp. 1–7. ASME, New York (1980).
2. J. K. Eaton and J. P. Johnson, A review of research on subsonic turbulent flow reattachment, *AIAA J.* **19**, 1093–1100 (1981).
3. R. L. Simpson, A review of some phenomena in turbulent flow separation, *J. Fluid Engng* **103**, 520–530 (1981).
4. B. F. Armaly, F. Durst, J. C. F. Pereira and B. Schounung, Experimental and theoretical investigation of backward-facing step flow, *J. Fluid Mech.* **127**, 473–496 (1983).
5. W. Aung, An experimental study of laminar heat transfer downstream of backsteps, *J. Heat Transfer* **105**, 823–829 (1983).
6. W. Aung, Separated forced convection, *Proc. ASME/JSME Thermal Engng Joint Conf.*, Vol. 2, pp. 499–515. ASME, New York (1983).
7. W. Aung, A. Baron and F. K. Tsou, Wall independency and effect of initial shear-layer thickness in separated flow and heat transfer, *Int. J. Heat Mass Transfer* **28**, 1757–1771 (1985).
8. W. Aung and G. Worku, Theory of fully developed, combined convection including flow reversal, *J. Heat Transfer* **108**, 485–488 (1986).
9. E. M. Sparrow, G. M. Chrysler and L. F. Azevedo, Observed flow reversals and measured-predicted Nusselt numbers for natural convection in a one-sided heated vertical channel, *J. Heat Transfer* **106**, 325–332 (1984).
10. E. M. Sparrow, S. S. Kang and W. Chuck, Relation between the points of flow reattachment and maximum heat transfer for regions of flow separation, *Int. J. Heat Mass Transfer* **30**, 1237–1246 (1987).
11. E. M. Sparrow and W. Chuck, PC solutions for heat transfer and fluid flow downstream of an abrupt, asymmetric enlargement in a channel, *Numer. Heat Transfer* **12**, 19–40 (1987).

CONVECTION MIXTE DANS DES ECOULEMENTS VERTICAUX DERRIERE UN ELARGISSEMENT SELON UNE MARCHE

Résumé—On présente des résultats sur la convection thermique mixte laminaire bidimensionnelle dans un canal vertical avec un élargissement selon une marche. L'étude numérique considère un large domaine de conditions d'écoulement interne et de température pariétale pour couvrir le domaine depuis la convection forcée pure jusqu'à la convection où les effets des forces de flottement sont significatifs et où la vitesse moyenne d'entrée est plus petite que la valeur correspondante de convection naturelle. Les résultats se comparent bien avec les données existantes, mais limitées, expérimentales et numériques. Cette étude considère une marche tournée vers l'aval avec un élargissement de 2, mais les comportements généraux observés sont applicables à des géométries semblables avec différents rapports d'élargissement. L'écoulement induit par le flottement diminue la longueur de recollement et éloigne la région de recirculation de la paroi chauffée. Des distributions de vitesse et de température ainsi que des nombres de Nusselt et des coefficients de frottement sont présentés pour de larges domaines des paramètres d'écoulement et de température.

MISCHKONVEKTION BEI AUFTRIEBSUNTERSTÜTZTER SENKRECHTER STRÖMUNG ENTLANG EINER STUFENFÖRMIG ZURÜCKWEICHENDEN WAND

Zusammenfassung—Es wird über den Wärmeübergang bei Mischkonvektion in laminarer auftriebsunterstützter zweidimensionaler Strömung in einem senkrechten Kanal mit stufenförmig zurückweichenden Wänden berichtet. Diese numerische Untersuchung deckt einen weiten Bereich von Eintrittszuständen von Strömung und Wandtemperatur ab. Der Bereich umfaßt damit ebenso die reine erzwungene Konvektionsströmung (ohne freie Konvektion) wie die schleichende Konvektionsströmung am Eintritt, wo die Auftriebseffekte spürbar sind und wo die mittlere Eintrittsgeschwindigkeit kleiner ist als im entsprechenden Fall der natürlichen Konvektion. Die Ergebnisse stimmen recht gut mit den in begrenztem Umfang vorhandenen Versuchsdaten und anderen numerischen Ergebnissen überein. Besonderes Augenmerk wird auf die Geometrie der zurückspringenden Stufen mit einem Erweiterungsverhältnis von 2 verwandt, das beobachtete allgemeine Verhalten kann jedoch auch auf ähnliche Geometrien mit abweichenden Erweiterungsverhältnissen angewandt werden. Die auftriebsinduzierte Strömung verkürzt die Länge bis zum Wiederanlegen und drückt die Rezirkulationszone von der beheizten Wand weg. Schließlich werden Geschwindigkeits- und Temperaturverteilungen zusammen mit der Nusselt-Zahl und den Widerstandsbeiwerten für weite Strömungs- und Temperaturbereiche dargestellt.

СМЕШАННАЯ КОНВЕКЦИЯ ПРИ ВЕРТИКАЛЬНОМ ТЕЧЕНИИ С ВНЕЗАПНЫМ СУЖЕНИЕМ ПРИ НАЛИЧИИ ПОДЪЕМНЫХ СИЛ

Аннотация—Представлены результаты смешанноконвективного теплопереноса в процессе ламинарного двумерного течения в вертикальном канале с внезапным сужением при действии подъемных сил. Численно исследуется широкий диапазон условий течения на входе и температур стенки, охватывающий область от чисто вынужденного конвективного течения, при котором отсутствуют эффекты подъемных сил, до вырождающегося конвективного течения на входе, при котором, данные эффекты существенны и средняя скорость на входе меньше, чем скорость естественной конвекции. Полученные результаты удовлетворительно согласуются с имеющимися, хотя и ограниченными экспериментальными и численными данными. Основное внимание уделяется случаю канала с коэффициентом расширения 2, однако установленные общие особенности течения применимы к аналогичным геометриям с другими коэффициентами расширения. Обусловленное подъемными силами течение вызывает сокращение длины отрывной зоны и удаление рециркулирующей области от нагретой стенки. Приводятся распределения скоростей и температур, а также значения числа Нуссельта и коэффициентов трения на стенке для широкого диапазона параметров течения и температуры.